Frequency-Domain Identification of Linear Time-Periodic Systems Using LTI Techniques

Matthew S. Allen
Assistant Professor
Department of Engineering Physics,
University of Wisconsin-Madison,
Madison, WI 53706
e-mail: msallen@engr.wisc.edu

A variety of systems can be faithfully modeled as linear with coefficients that vary periodically with time or linear time-periodic (LTP). Examples include anisotropic rotor-bearing systems, wind turbines, and nonlinear systems linearized about a periodic trajectory. Many of these have been treated analytically in the literature, yet few methods exist for experimentally characterizing LTP systems. This paper presents a set of tools that can be used to identify a parametric model of a LTP system, using a frequency-domain approach and employing existing algorithms to perform parameter identification. One of the approaches is based on lifting the response to obtain an equivalent linear time-invariant (LTI) form and the other based is on Fourier series expansion. The development focuses on the preprocessing steps needed to apply LTI identification to the measurements, the postprocessing needed to reconstruct the LTP model from the identification results, and the interpretation of the measurements. This elucidates the similarities between LTP and LTI identification, allowing the experimentalist to transfer insight between the two. The approach determines the model order of the system and the postprocessing reveals the shapes of the time-periodic functions comprising the LTP model. Further postprocessing is also presented, which allows one to generate the state transition and time-varying state matrices of the system from the output of the LTI identification routine, so long as the measurement set is adequate. The experimental techniques are demonstrated on simulated measurements from a Jeffcott rotor mounted on an anisotropic flexible shaft supported by anisotropic bearings. [DOI: 10.1115/1.3187151]

Keywords: Floquet theory, Floquet exponent, Floquet multiplier

1 Introduction

Many important dynamic systems can be modeled as linear time-periodic (LTP), and it is exceedingly important to discover and accurately model this character since such a system can exhibit parametric resonances, which are not present for a linear time-invariant (LTI) approximation to the system. Floquet [1] initiated the study of LTP systems in the 1800s, and the Floquet theory has been applied to a variety of mechanical systems such as helicopters and wind turbines. Linear time-periodic systems are also frequently encountered when a nonlinear system is linearized about a periodic trajectory.

Much progress has been made toward the analysis and control of time-periodic systems, yet experimental identification of LTP systems has received relatively little attention. Many texts cover system identification approaches for general time-varying systems, but most of those are not appropriate for LTP systems with rapidly varying parameters. Two early works that overcame these limitations are the subspace methods of Hench [2] and Verhaegen and co-workers [3,4]. Liu presented a similar method in Ref. [5] (see Ref. [6]) that is applicable to LTP systems. Peters and Wang [7] independently arrived at a related methodology, and applied their technique to find the Floquet multipliers of a laboratory helicopter rotor [8]. All of these are time-domain methods and focus on the discrete-time representation for a LTP system, and none proposed on how one might recover the continuous-time system matrices from the discrete-time model that they identify, yet this is of interest in many applications.

In many instances frequency-domain approaches are preferred [9], but few have been developed for LTP systems. Wereley and Hall [10] and Siddiqui [11] developed the concept of harmonic transfer functions (HTFs) to treat LTP systems in the frequency domain, and their methods were recently applied to measurements from a wind tunnel model of a helicopter rotor [12], although no meaningful time-periodic behavior could be detected. A number of other methods also exist, which are applicable to both nonlinear and LTP systems, although most are limited to single degree of freedom or low order systems [13].

This work presents a frequency-domain approach that allows one to characterize a LTP system using the same methodology, algorithms, and intuition that are used for LTI systems. The focus is on developing the pre- and postprocessing needed so that any suitable LTI identification routine can be used to process free response measurements from a LTP system. Particular emphasis is placed on finding the proper model order and on correctly distinguishing time-periodic behavior from noise, signal processing errors, and other factors that are common to experimental measurements. The model order is identified by interrogating the response data, as is done for LTI systems, and nothing is assumed about the model form except that it is linear and time-periodic. When the fundamental period of the system is known, a lifting scheme [3,14] is used to transform the measurements into a set of responses that can be described by a LTI model. A Fourier series description is also developed, which can, in principle, be used to address the case where the fundamental period is not known, and which is the converse of the HTF approach [10,11]. This work also shows how one can estimate the state transition matrix (STM) and the time-varying state matrix of the system if an adequate set of responses has been collected. These methods have recently

Contributed by the Design Engineering Division of ASME for publication in the JOURNAL OF COMPUTATIONAL AND NONLINEAR DYNAMICS. Manuscript received December 28, 2007; final manuscript received December 31, 2008; published online August 24, 2009. Review conducted by Subhash C. Sinha. Paper presented at the ASME 2007 Design Engineering Technical Conferences and Computers and Information in Engineering Conference (DETC2007), Las Vegas, NV, September 4–7, 2007.

been applied to identify LTI structural modes from continuous-scan laser vibrometer measurements [15–18], where the LTP response has many modes with complicated time-periodic patterns, so the aforementioned features have proved highly beneficial.

2 Theoretical Development

Section 2.1 briefly reviews some pertinent concepts from the Floquet theory. Section 2.2 presents two descriptions that can be used to identify parametric models of LTP systems using LTI methods, and Sec. 2.3 describes how to reconstruct the LTP state transition matrix and state matrix from the parametric model.

2.1 Review of Floquet Theory for LTP Systems. The response of a linear time-varying system,

$$\dot{x} = A(t)x$$

$$y = C(t)x \tag{1}$$

where x is the $N\times 1$ system state vector, y is the $N_o\times 1$ vector of the outputs, and the matrices $A(t)$ and $C(t)$ are periodic with period T_A (e.g., $A(t+T_A)=A(t)$), which is related to its initial state $x(t_0)$ by its state transition matrix,

$$x(t) = \Phi(t,t_0)x(t_0) \tag{2}$$

Floquet's theorem [19] states that if the state transition matrix is diagonalizable, then it can be decomposed as

$$\Phi(t,t_0) = \Psi(t)\exp(\Lambda_R(t-t_0))\Psi(t_0)^{-1} \tag{3}$$

where $\Psi(t)=[\{\psi_1\},\ldots,\{\psi_N\}]$ is the periodic modal matrix of the STM, and Λ_R is a diagonal matrix containing the Floquet exponents of the system. The Floquet multipliers μ_r are related to the Floquet exponents λ_r by $\mu_r=\exp(\lambda_r T_A)$, but the latter can be determined from μ_r only up to an arbitrary integer n

$$\lambda_r = \frac{\ln(\mu_r)}{T_A} + in\omega_A \tag{4}$$

where $\omega_A=2\pi/T_A$. This is of little consequence because one can correctly reconstruct the STM in Eq. (3) with any n, and likewise, all of the following is valid for any n. However, as the strength of the system's time-periodicity decreases, the mode vectors $\{\psi_r(t)\}$ reduce to constant vectors only for a specific n.

The response of the system, after expressing Eq. (3) in summation form, is given by

$$y(t) = \sum_{r=1}^{N} R_Y(t)_r \exp(\lambda_r(t-t_0))$$

$$R_Y(t)_r = C(t)\{\psi_r(t)\}\{L_r(t_0)\}^T\{x_0\} \tag{5}$$

where $R_Y(t)_r$ is the periodic residue vector of the observed response, and $\{L_r(t_0)\}^T$ is the rth row of $\Psi(t_0)^{-1}$.

2.2 Identifying Parametric Models for LTP Systems

2.2.1 Lifting Approach. Consider the response in Eq. (5), sampled P times per fundamental period and over N_c cycles, where $N_c=N_s/P$ and both N_c and P are integers. The periodicity of $R_Y(t)_r$ is not observed if one always samples at the same point within the fundamental period, and so the response becomes a superposition of exponentials with constant amplitudes. This idea has been used for analysis [4,20,21], where it was called "lifting." The lifted response at the mth time instant is

$${y_m}^L = [{y_0}^T, {y_1}^T, \cdots, {y_{P-1}}^T]^T \tag{6}$$

where y_k is the response at t_n for $n=k+mP$ and m ranges from 0 to N_c-1.

The free response of the lifted system has the following form:

$${y_m}^L = \sum_{r=1}^{N} {R^{Ld}}_r \exp(\lambda_r m T_A) \tag{7}$$

where the kth block of rows in ${R^{Ld}}_r$ is

$${R^{Ld}}_{k,r} = R_Y(t_k)_r \exp(\lambda_r(t_k-t_0)) \tag{8}$$

The exponential term is important because it accounts for the delay between t_0 and the beginning of each response y_k. For convenience, we also define ${R^L}_r$, which is identical to ${R^{Ld}}_r$ but without the exponential term, and is the lifted form of $R_Y(t)_r$. Equation (7) has the same form as the response of a LTI system, so LTI parameter identification routines can be applied either to $y^L(t)$ or to its frequency domain dual.

$$Y^L(\omega) = \sum_{r=1}^{N} \frac{{R^{Ld}}_r}{i\omega - \lambda_r} \tag{9}$$

In either case, a LTI algorithm can be used to extract ${R^{Ld}}_r$ and λ_r from the responses. One can then estimate ${R^L}_r$ by multiplying each block of ${R^{Ld}}_r$ by $\exp(-\lambda_r(t_k-t_0))$. Note that this multiplication involves the identified Floquet exponents, whose imaginary part contains an arbitrary integer multiple of ω_A. This may cause the Fourier series expansion of ${R^L}_r$ to be shifted by an arbitrary amount from the description that one might expect for a time-invariant approximation to the system.

By analogy with LTI systems, measurements from N_i different initial conditions can be considered to form an $N_o\times N_i$ matrix of responses at each frequency, in which case it follows from the definition of ${R^{Ld}}_r$ that the resulting residue matrices are rank-one, each column being proportional to the mode vectors $C(t_k)\times\{\psi_r(t_k)\}$ just as for a LTI system. Hence, concepts such as the mode indicator function [22] and multi-input-multi-output (MIMO) identification, which are important tools for detecting close natural frequencies [22], are directly applicable. If P is large, then there will be a large number of outputs and one should seek an algorithm that can efficiently handle them; this work uses the algorithm of mode isolation (AMI) [23], which considers all of the responses simultaneously to obtain the best global estimate of the Floquet exponents.

One important difference between the identification of the lifted LTP system and standard LTI identification is that the bandwidth of $Y^L(\omega)$ is limited to half of ω_A, which may alias the lifted response. In that case, one can account for the aliasing using the sampled (star*) Laplace transformation [14], which is equivalent to fitting the response to a model with z-domain polynomials (i.e., replace $i\omega$ in Eq. (9) with $z=\exp(i\omega T_A)$). However, the distinction is usually not important for lightly damped structures if the Floquet exponents are not too close to 0 or $\omega_A/2$.

2.2.2 FSE Method. Because the residues $R_Y(t)_r$ in Eq. (5) are periodic, they can be readily expanded in a Fourier series. Here we shall presume that they can be adequately represented using a fixed number $(2N_R+1)$ of terms so that the response may be written as

$$y(t) = \sum_{r=1}^{N}\left(\sum_{m=-N_R}^{N_R} B_{r,m}\exp(im\omega_A(t-t_0))\right)\exp(\lambda_r(t-t_0)) \tag{10}$$

where $B_{r,m}$ is the mth complex Fourier coefficient of the rth residue. Factoring out the summations reveals the nature of the response

$$y(t) = \sum_{r=1}^{N} \sum_{m=-N_R}^{N_R} B_{r,m} \exp((\lambda_r + im\omega_A)(t - t_0)) \tag{11}$$

which is equivalent to that of a LTI system with $N(2N_R+1)$ eigenvalues $\lambda_r + im\omega_A$. The amplitude of each pseudomode in the response is determined by the Fourier coefficient $B_{r,m}$ that defines its residue. In light of Eq. (11) one can identify the parameters of a LTP system by processing its free response directly using a LTI system identification algorithm; that equation then allows one to interpret the result and reconstruct the LTP representation.

2.2.3 Comparison and Discussion. The most important distinction between these two approaches is that the lifting method represents the response with many additional outputs while the Fourier series expansion (FSE) method uses many modes. The lifting approach is advantageous in this regard because the difficulty and potential for ill-conditioning in most system identification routines scale with the number of poles in the response, while response points are easy to accommodate [22]. The responses obtained by the lifting method are also easier to interpret—the system's model order is readily apparent. Furthermore, rigorous application of the FSE method requires a customized approach because standard LTI system identification routines do not enforce the spacing between the eigenvalues that Eq. (11) requires. This is an advantage if ω_A is not known, as one might be able to determine it from a collection of identified eigenvalues. On the other hand, when ω_A is known the lifting method allows one to globally [22] identify the Floquet exponents of the system, utilizing all of the responses simultaneously, and one can always find an equivalent FSE representation by applying a discrete Fourier transform (DFT) to R^L_r.

2.3 Postprocessing. This section presents the postprocessing operations that extract the state transition matrix or the time-varying state matrix from the parameters $B_{r,m}$ and λ_r identified using the procedure just outlined. The STM and state matrix are easiest to interpret if the set of output points is sufficient to define a unique state, so the following assumes that this is the case. If that condition is not met, then one can augment the state vector with measurements from later time steps, as done in Ref. [7].

2.3.1 Reconstructing the State Transition Matrix. The following assumes that the measured outputs uniquely define the displacement state of the system through a known, full-rank, constant matrix E via

$$x_d(t) = Ey(t) \tag{12}$$

which is only possible if there are more measurement locations than states. Once the model order is identified, an adequate state vector can be formed, e.g., by choosing a subset of the outputs using a Boolean matrix E.

If the system is a second-order structural dynamic system, then one can use the derivatives of the displacement states to find the velocity states, so the final state vector is $x(t) = [x_d(t)^T, dx_d(t)/dt^T]^T$.

In terms of the state vector just defined, the residues are $(B_x)_{r,m} = EB_{r,m}$, so

$$x_d(t) = \sum_{r=1}^{2N} \sum_{m=-N_R}^{N_R} (B_x)_{r,m} \exp((\lambda_r + im\omega_A)(t - t_0)) \tag{13}$$

and one can differentiate to obtain the velocity states as

$$x_v(t) = \sum_{r=1}^{2N} \sum_{m=-N_R}^{N_R} (B_x)_{r,m} (\lambda_r + im\omega_A) \exp((\lambda_r + im\omega_A)(t - t_0)) \tag{14}$$

One must assure that the identified response model is reliable, because the differentiation required could amplify errors in the components for large m, but this can be avoided if the acceleration or velocity is measured in lieu of displacement.

One now has a FSE model for the state response $x(t)$ due to some initial condition $x(t_0)$, which is known by evaluating the FSE model at $t = t_0$. Hence, the only unknown in Eq. (2) is the state matrix. However, there are N^2 unknowns in the state matrix at each time step and only one response due to one length N initial condition. Fortunately, one can generate the required responses by shifting each response by nT_A, where n is an integer. Because the residues are periodic, $x(t+nT_A)$ is equal to $x(t)$ with each term in the summation of the latter multiplied by $\exp(\lambda_r nT_A)$, so we can form the following system of linear equations:

$$\begin{bmatrix} x(t) & \cdots & x(t + (N-1)T_A) \end{bmatrix} = \Phi(t, t_0) \begin{bmatrix} x(t_0) & \cdots & x(t_0 + (N-1)T_A) \end{bmatrix} \tag{15}$$

The matrix multiplying the STM on the far right is a known constant matrix of initial conditions, which is denoted by $[x_{IC}]$, and after solving for the STM and after inserting Eqs. (13) and (14), we obtain

$$\Phi(t, t_0) = \sum_{r=1}^{N} \sum_{m=-N_R}^{N_R} \begin{Bmatrix} (B_x)_{r,m} \\ (B_x)_{r,m}(\lambda_r + im\omega_A) \end{Bmatrix} \begin{bmatrix} 1 & \cdots & \exp(\lambda_r NT_A) \end{bmatrix} \times [x_{IC}]^{-1} \exp((\lambda_r + im\omega_A)(t - t_0)) \tag{16}$$

It is now apparent that one can take

$$\{\psi_r(t)\} = \sum_{m=-N_R}^{N_R} \begin{Bmatrix} (B_x)_{r,m} \\ (B_x)_{r,m}(\lambda_r + im\omega_A) \end{Bmatrix} \exp(im\omega_A(t - t_0)) \tag{17}$$

and

$$\{L_r(t_0)\}^T = \begin{bmatrix} 1 & \cdots & \exp(\lambda_r NT_A) \end{bmatrix} [x_{IC}]^{-1} \tag{18}$$

to obtain a valid construction of the state transition matrix.

2.3.2 Time-Periodic State Matrix. Once a FSE model for the state transition matrix has been identified, one can use the STM differential equation

$$\frac{d}{dt}\Phi(t, t_0) = A(t)\Phi(t, t_0) \tag{19}$$

to solve for the time-varying system matrix $A(t)$ as

$$A(t) = \left(\frac{d}{dt}\Phi(t, t_0) \right) \Phi(t, t_0)^{-1} \tag{20}$$

In the applications that follow, this was accomplished numerically at each time step t_k in the interval $[0, T_A)$. The derivative of the STM was found by differentiating Eq. (16), as was done for the response model in Eq. (14).

3 Simulated Application

The proposed system identification methods were evaluated by applying them to simulated measurements from a LTP system representing a Jeffcott rotor on an anisotropic shaft (Fig. 1). A lumped parameter model is also shown, consisting of a point mass suspended by two orthogonal, massless springs with spring constants k_{Rx} and k_{Ry}. The springs are attached to a massless turntable that turns at constant speed Ω. The turntable is fixed to ground by two massless springs k_{Fx} and k_{Fy}. Defining nondimensional time as $t = \omega_n t'$, where $\omega_n = \sqrt{k_{Fx}/m}$, the following equations of motion were obtained in the fixed reference frame

$$[I] \begin{Bmatrix} \ddot{X} \\ \ddot{Y} \end{Bmatrix} + [\hat{C}] \begin{Bmatrix} \dot{X} \\ \dot{Y} \end{Bmatrix} + [\hat{K}(t)] \begin{Bmatrix} X \\ Y \end{Bmatrix} = \begin{Bmatrix} 0 \\ 0 \end{Bmatrix}$$

$$[\hat{C}] = \omega_n c_f [\hat{K}_F], \quad [R(t)] = \begin{bmatrix} \cos(\hat{\Omega}t) & \sin(\hat{\Omega}t) \\ -\sin(\hat{\Omega}t) & \cos(\hat{\Omega}t) \end{bmatrix}, \quad \hat{\Omega} = \frac{\Omega}{\omega_n}$$

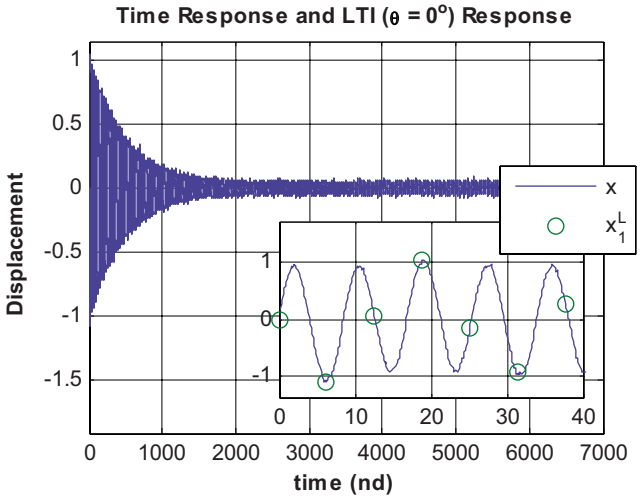

Fig. 2 Noise contaminated time response of a LTP system with circles showing the first lifted response y^L_1

$$[\hat{K}(t)] = [R][\hat{K}_R][R]^T([I] - ([R][\hat{K}_R][R]^T + [\hat{K}_F])^{-1}[R][\hat{K}_R][R]^T)$$

$$[\hat{K}_R] = \begin{bmatrix} k_{Rx}/k_{Fx} & \\ & k_{Ry}/k_{Fx} \end{bmatrix}, \quad [\hat{K}_F] = \begin{bmatrix} 1 & \\ & k_{Fy}/k_{Fx} \end{bmatrix} \tag{21}$$

The following parameters are used in the following: $k_{Rx}/k_{Fx}=1$, $k_{Ry}/k_{Fx}=1.5$, $c_f=0.004$, $k_{Fy}/k_{Fx}=2$, and $\hat{\Omega}=0.5$. The equations of motion are periodic with period $T_A=2\pi$, which corresponds to one-half of a revolution of the shaft. The natural frequencies of the system with the shaft held fixed at various angles ranged from 0.707 rad/s to 0.926 rad/s. Stability analysis was performed using the method in Ref. [24], revealing that the system is unstable for $0.72<\hat{\Omega}<0.755$, $0.785<\hat{\Omega}<0.825$, and $0.848<\hat{\Omega}<0.92$, so it would certainly be important to detect and properly characterize this system's time-periodicity if it is to operate at high speeds.

The response of the system to a unit impulsive force was found using adaptive time integration with $\Delta t=0.126$ (50 samples per half revolution of the shaft), and for 512 revolutions so that the response decayed to a small fraction of its initial amplitude.

Measurements were simulated of the displacements of the mass and of the turntable (tt) in the fixed frame and in both directions, so the output vector is $y=[X^T,Y^T,X_{tt}{}^T,Y_{tt}{}^T]^T$. The turntable is massless, so its displacement is related to that of the mass by a time-varying transformation. This mimics the case where one might measure at multiple points on a flexible system, not knowing a priori how many points are required to capture the modes of the system. The response was contaminated with Gaussian white noise, whose standard deviation was equal to 2% of the maximum response in each coordinate, to simulate a more realistic scenario.

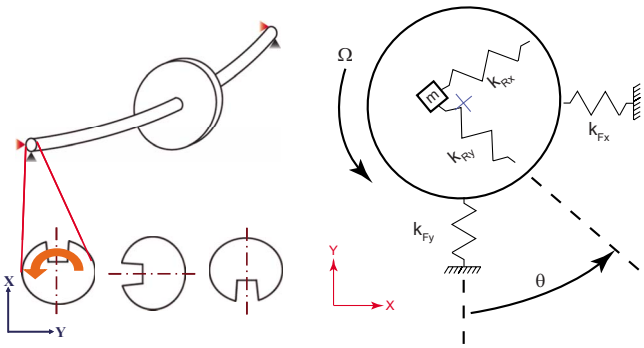

Fig. 1 (Left) illustration of a rotor on an anisotropic shaft and bearings; (right) lumped parameter schematic of the LTP system

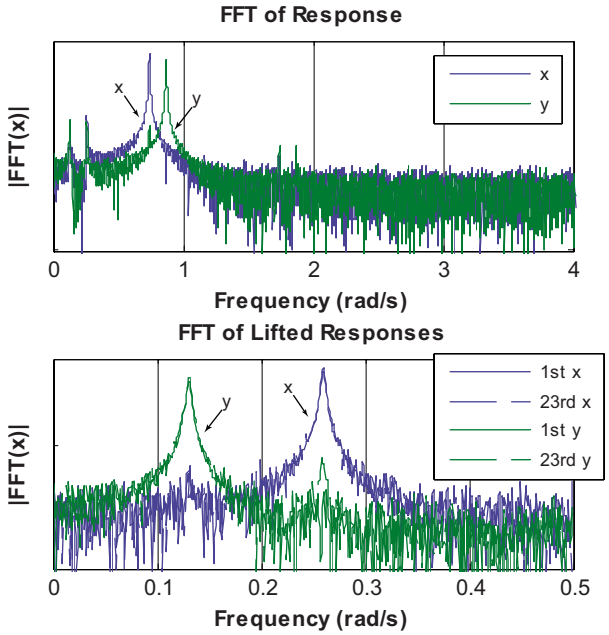

Fig. 3 Responses of mass in *X* and *Y*: (top) DFT of time response and (bottom) DFT of two of the lifted responses

3.1 Response Model Identification. Figure 2 shows the noise contaminated time response of the output $y_1=X$ and markers highlight the response points at which the shaft (or turntable) is at either 0 deg or 180 deg, which corresponds to the first element of the lifted response $y^L{}_1$, showing that the lifted response aliases the true response frequency.

The DFT of the outputs is shown in the upper panes in Figs. 3 and 4, for X and Y and for X_{tt} and Y_{tt}, respectively. The response

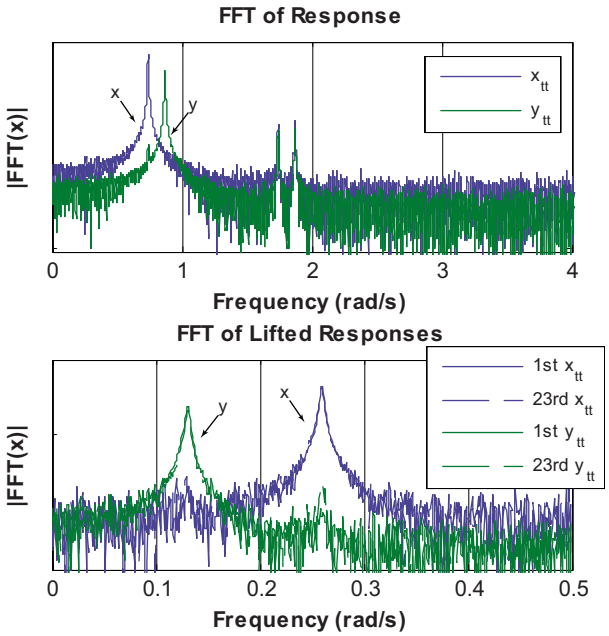

Fig. 4 Responses of turntable X_{tt} and Y_{tt}: (top) DFT of time response and (bottom) DFT of two of the lifted responses

in all of the outputs is dominated by two resonant peaks surrounding at 0.8 rad/s. Figure 3 shows two other pairs of peaks at 0.2 rad/s and 1.8 rad/s, although the latter are almost completely masked by the noise. In contrast, Fig. 4 shows noticeable harmonics only at 1.8 rad/s. In any event, this two degree of freedom LTP system appears to have at least six active modes in this response, the reason for which was explained by Eq. (11).

The response was also decomposed according to the lifting method, and the DFT of the lifted responses was found, two of which are shown in the bottom panes in Figs. 3 and 4. The first and 23rd responses are shown corresponding to instances when the shaft was at 0 deg or 180 deg (first) and 79.2 deg or 259.2 deg (23rd). Each DFT shows at most two resonant peaks, and the amplitude of the peaks is somewhat different in each of the responses shown, and indeed differed between all 50 lifted responses as expected.

The set of 200 lifted responses were processed using the algorithm of mode isolation [23], which considered all 200 responses simultaneously, automatically identifying both of the modes of the system and their residues, and the algorithm automatically determined the model order by observing that the response was reduced to noise after removing these modal contributions from the data. The identified Floquet exponents were

$$(\lambda_{\text{ident}})_1 = -0.002051 + i0.1302$$

$$(\lambda_{\text{ident}})_2 = -0.002036 + i0.2594$$

The Floquet exponents were also computed numerically [24], and the following values were obtained, which agree quite closely with those shown above:

$$(\lambda_{\text{analytical}})_1 = -0.002000 + i0.13034$$

$$(\lambda_{\text{analytical}})_2 = -0.002000 + i0.25939$$

3.2 State Transition and System Matrices. Two modes have been identified from the four responses for this system, so we can use the methods in Sec. 2.3 to find the STM and time-varying state matrix of the system for a subset of the responses. The responses X and Y were used to do this, so E in Eq. (12) is a 2×4 matrix with $E_{11}=E_{22}=1$ and all other elements as zero. The residues identified by AMI were converted to a FSE model by applying a DFT, and the top pane in Fig. 5 displays the absolute value of each of the coefficients of a DFT of the lifted residue for mode 1, X-coordinate. Only three terms stand out significantly above the noise for this residue, and the same was true for all of the other residues. The other coefficients are on the order of random fluctuations due to the artificially added noise, so they were discarded. The residue was reconstructed using the three retained Fourier coefficients, and its real and imaginary parts are shown as a function of the shaft angle in the bottom pane, revealing that it follows the general trend of the identified residue but is much smoother.

The retained Fourier coefficients were then used to reconstruct the state transition matrix. The $(B_x)_{r.m}$ coefficients defined the Floquet mode shapes $\{\psi(t)\}$, and the procedure described was used to find $\{L_r(t_0)\}$, completing the model for the STM. The derivative of the STM was also found, both were evaluated at 50 time instants over the fundamental period, and Eq. (20) was then used to solve for $A(t)$ at each time instant.

Figure 6 shows three of the coefficients of the state matrix that were estimated using this procedure, as compared with the actual analytical coefficients. The $A(3,1)$ $A(3,2)$, and $A(3,3)$ coefficients that are shown correspond to the negatives of the (1,1) and (1,2) elements of the stiffness matrix and the (1,1) element of the damping matrix for this system, respectively. As expected, at $\theta=0$ the K_{11} term is equal to $-0.5=-(k_{Rx}*k_{Fx})/(k_{Rx}+k_{Fx})$, which is the series stiffness of the system at that angle. The K_{12} term is zero for $\theta=0$ and increases to a maximum negative value at 45 deg. The identified terms reveal that the stiffness matrix is sinusoidal, the dominant terms being the constant term, followed by terms that have one period per half revolution of the shaft. The (1,1) element of the damping matrix is much smaller than the stiffness terms. It is significant to note that this system matrix was estimated without a priori knowledge of either the system order or of the form of its time-varying functions.

All three of the coefficients of $A(t)$ were accurately estimated

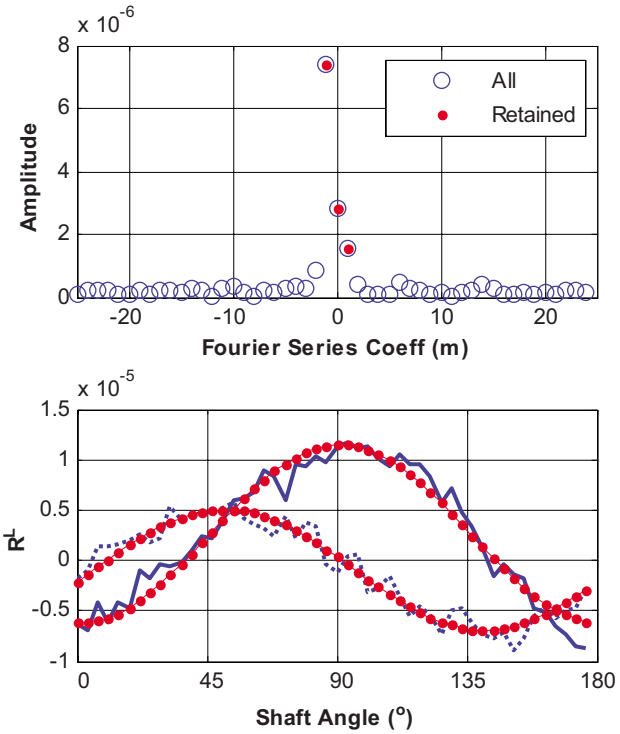

Fig. 5 (Top) DFT of *X*-component of the residue vector for mode 1. Circles show all 50 DFT coefficients, points indicate the coefficients that were retained. (Bottom) Plot of residue for mode 1. Lines show the real (solid) and imaginary (dashed) parts of the residue found by AMI, while red circles show the reconstruction of the real and imaginary parts using the indicated coefficients.

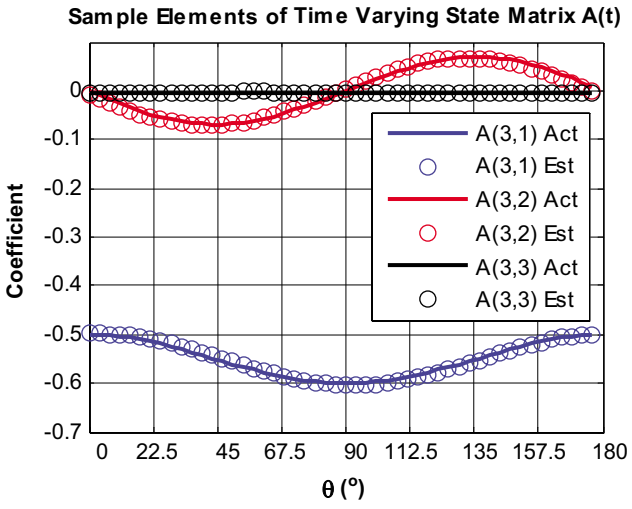

Fig. 6 Sample coefficients of the time-varying system matrix $A(t)$: (solid) actual coefficient as a function of shaft angle and (circles) coefficient estimated from noise contaminated response data

using the proposed procedure. The maximum error in any coefficient over all shaft angles was 0.013. This corresponds to 1.3% error since the largest coefficient in $A(t)$ is 1. However, the terms in the portion of $A(t)$ corresponding to the damping matrix are small, so the errors in those terms are almost 100% of their actual maximum values. To evaluate the sensitivity of the results to the choice of state variables for this system, the same procedure was also repeated with X_{tt} and Y_{tt} selected as the states. Once again three Fourier coefficients were found to be sufficient to describe the identified residues. The $A(t)$ matrix estimated in that case was compared with that derived for the system, and the largest error found was 3.1% in the coupling stiffness between X_{tt} and Y_{tt}.

3.3 Discussion. This paper has mimicked an actual experiment using simulated noise, which masks all but a few of the peaks in the spectrum shown in the top pane in Figs. 3 and 4. When the lifting method is used, measurement noise makes the residues of the state transition matrix more jagged than they would otherwise be. While these residues can be used to accurately reconstruct the response, one does encounter difficulty when using them to reconstruct the time-varying state matrix $A(t)$ due to the differentiation required. This difficulty was overcame by eliminating all of the Fourier coefficients that did not stand out above the noise floor. For this system, the $A(t)$ matrix was accurately estimated using various collections of the identified Fourier coefficients (the three dominant ones were used to create Fig. 6), although the error in $A(t)$ increased if too many were used. For example, if all coefficients for $-3 \leq m \leq 3$ were retained, the maximum error in $A(t)$ increased to 6.2% and the estimate of the state matrix showed artificial waviness. In general, one must design an experiment such that all important Fourier coefficients stand out above the noise or erroneous results may be obtained.

4 Conclusions

A methodology was presented by which one can identify a response model, the time-varying state matrix, and the state transition matrix of a linear time-periodic system from free response measurements. A series of pre- and postprocessing steps were presented so that virtually any system identification algorithm for multi-output LTI systems can be used, and some guidelines were presented to aide in selecting an algorithm. The proposed approach was demonstrated using synthesized, noise contaminated response data, and the proposed lifting method was found to simplify the process of identifying the Floquet exponents of the LTP system and its model order; a standard system identification routine for LTI systems was able to automatically identify the modes in the response and in the model order. This revealed that a subset of the measurement points was sufficient to describe the displacement state of the system, and two different subsets of the measurement points were used to find the system's state transition matrix $\Phi(t, t_0)$ and its time-periodic system matrix $A(t)$. Each term in the system matrix was estimated within a few percent in both cases, in spite of the measurement noise.

References

[1] Floquet, G., 1883, "Sur Les Equations Lineaires a Coefficients Periodiques," Ann. Sci. Ec. Normale Super., **12**(2), pp. 47–88.

[2] Hench, J. J., 1995, "A Technique for the Identification of Linear Periodic State-Space Models," Int. J. Control, **62**(2), pp. 289–301.

[3] Verhaegen, M., and Xiaode, Y., 1995, "A Class of Subspace Model Identification Algorithms to Identify Periodically and Arbitrarily Time-Varying Systems," Automatica, **31**(2), pp. 201–216.

[4] Felici, F., van Wingerden, J. W., and Verhaegen, M., 2007, "Subspace Identification of MIMO LPV Systems Using a Periodic Scheduling Sequence," Automatica, **43**(10), pp. 1684–1697.

[5] Liu, K., 1997, "Identification of Linear Time-Varying Systems," J. Sound Vib., **206**(4), pp. 487–505.

[6] Shi, Z. Y., Law, S. S., and Li, H. N., 2007, "Subspace-Based Identification of Linear Time-Varying System," AIAA J., **45**(8), pp. 2042–2050.

[7] Peters, D. A., and Wang, X., 1998, "Generalized Floquet Theory for Analysis of Numerical or Experimental Rotor Response Data," 24th European Rotorcraft Forum, Marseilles, France, Sept. 15–17.

[8] Fuehne, C. P., 2000, "Application of Generalized Floquet Theory to Numerical and Experimental Data," Ph.D. thesis, Washington University in St. Louis, St. Louis, MO.

[9] Pintelon, R., and Schoukens, J., 2001, *System Identification: A Frequency Domain Approach*, IEEE, Piscataway, NJ.

[10] Wereley, N. M., and Hall, S. R., 1991, "Linear Time Periodic Systems: Transfer Functions, Poles, Transmission Zeroes and Directional Properties," *Proceedings of the 1991 American Control Conference*, Boston, MA.

[11] Siddiqui, A., 1999, "Identification of the Harmonic Transfer Functions of a Helicopter Rotor," Ph.D. thesis, Massachusetts Institute of Technology, Cambridge, MA.

[12] Shin, S. J., Cesnik, C. E. S., and Hall, S. R., 2005, "System Identification Technique for Active Helicopter Rotors," J. Intell. Mater. Syst. Struct., **16**(11–12), pp. 1025–1038.

[13] Kerschen, G., Worden, K., Vakakis, A. F., and Golinval, J.-C., 2006, "Past, Present and Future of Nonlinear System Identification in Structural Dynamics," Mech. Syst. Signal Process., **20**, pp. 505–592.

[14] Luxemburg, L. A., 1990, "Frequency Analysis of Time-Varying Periodic Linear Systems by Using Modulo P Transforms and Its Applications to the Computer-Aided Analysis of Switched Networks," Circuits Syst. Signal Process., **9**(1), pp. 3–29.

[15] Allen, M., and Ginsberg, J. H., 2006, "Floquet Modal Analysis to Detect Cracks in a Rotating Shaft on Anisotropic Supports," 24th International Modal Analysis Conference (IMAC XXIV), St. Louis, MO, Jan. 30–Feb. 2.

[16] Allen, M. S., 2007, "Floquet Experimental Modal Analysis for System Identification of Linear Time-Periodic Systems," ASME 2007 International Design Engineering Technical Conference, Las Vegas, NV, Sept. 4–7.

[17] Allen, M. S., and Sracic, M. W., 2008, "A Method for Generating Pseudo Single-Point FRFs from Continuous Scan Laser Vibrometer Measurements," 26th International Modal Analysis Conference (IMAC XXVI), Orlando, FL, Feb.

[18] Allen, M. S., and Sracic, M. W., 2008, "Mass Normalized Mode Shapes Using Impact Excitation and Continuous-Scan Laser Doppler Vibrometry," Eighth International Conference on Vibration Measurements by Laser Techniques, Ancona, Italy.

[19] D'Angelo, H., 1970, "Linear Time-Varying Systems: Analysis and Synthesis," *Allyn and Bacon Series in Electrical Engineering*, Allyn and Bacon, Boston, MA.

[20] Meyer, R. A., and Burrus, C. S., 1975, "Unified Analysis of Multirate and Periodically Time-Varying Digital-Filters," IEEE Trans. Circuits Syst., **22**(3), pp. 162–168.

[21] Arambel, P. O., and Tadmor, G., 1994, "Robust H Infinity Identification of Linear Periodic Discrete-Time Systems," Int. J. Robust Nonlinear Control, **4**(4), pp. 595–612.

[22] Allemang, R. J., and Brown, D. L., 1998, "A Unified Matrix Polynomial Approach to Modal Identification," J. Sound Vib., **211**(3), pp. 301–322.

[23] Allen, M. S., and Ginsberg, J. H., 2006, "A Global, Single-Input-Multi-Output (SIMO) Implementation of the Algorithm of Mode Isolation and Applications to Analytical and Experimental Data," Mech. Syst. Signal Process., **20**, pp. 1090–1111.

[24] Friedmann, P., Hammond, C. E., and Woo, T.-H., 1977, "Efficient Numerical Treatment of Periodic Systems With Application to Stability Problems," Int. J. Numer. Methods Eng., **11**, pp. 1117–1136.